Preparation, Electrical and Modulation Optical Properties of 2H-MoSe₂

Ying-Sheng HUANG (黃鶯聲)

Department of Electronic Engineering and Technology
National Taiwan Institute of Technology, Taiwan, R.O.C.

A " two-step" halogen vapor transport method has been developed for growing large size single crystals of $MoSe_2$ of 2H form. The electrical and modulation optical properties are investigated in order to get a better understanding of its band structure. Conductivity measurements show that intrinsic conductivity begins to dominate at 650° K with a thermal energy gap around 1 eV. The optical properties are studied by thermoreflectance (TR) and electrolyte electroreflectance (EER) techniques in the range of 1.4 to 6.2 eV at room temperature. Both TR and EER spectrum exhibit sharp structures in the vicinity of the excitonic transitions A, B, A' and B' as well as higher lying interband transitions. A comparison of TR and EER spectrum helps *to* identify the various features in the spectra of these two different modulated techniques. The interband transition energies are then determined with a better accuracy.

---

1. INTRODUCTION

L AYERED compounds of the transition-metal dichalcogenide have been the subject of intensive theoretical and experimental studies because of their possible application as high temperature superconductors[ ], as solid superionic cathodes in new battery systems*, as a new class of electrodes for photoelectrochemical solar cells[3]; and because of their unusual anisotropic physical properties[4,5]. $MoSe_2$ is a member of this family of compounds which has not as extensively studied as MoS_2 because it is not as easily available.

MoS_2 is a semiconducting compound. The structure of 2H-$MoSe_2$ has sixfold trigonal prismatic coordination of the Mo atoms by the Se atoms within the layers, and there are *two* layers per unit cell stacked in hexagonal symmetry. The structure belongs to the space group D_{6h}^4. There is strong covalent bonding within the layers and weak Van der Waals-force between the layers. As a consequence, there is significant asymmetry (by a factor of 10^2 to 10^3) between the transport properites parallel and perpendicular to the layers. Crystals can be cleaved readily in very thin plates parallel to the layers perpendicular to the hexagonal c-axis.

Only relatively incomplete experimental information on its solid state properties have been

reported. In addition very little theoretical data exist on the band structure of $MoSe_2$ Several modulation spectroscopic methods[6-9] have been used to study the excitons A, B, A' and B' in the range 1.4 to 3 eV but little is known about the higher energy features. A complete understanding of the band structure is not possible without a detailed study of the higher energy interband transitions.

A "two-step" halogen vapor transport method has been developed for growing large size single crystals of 2H-MoSe$_2$. The temperature dependence of-conductivity has been studied between 135°K and 800° K by using a four probe potentiometric technique. Both thermoreflectance (TR) and electrolyte electroreflectance (EER) techniques have been employed to study the optical spectra of MoSe$_2$ in the range of 1.4 to 6.2 eV at room temperature. A comparison of TR.and EE' R spectrum helps to identify the various features in the spectra of these ' two techniques. The interband transition energies are then determined with a better accuracy than that achieved in the past. This gives a better understanding of the band structure of 2H-MoSe$_2$.

2. EXPERIMENTAL DETAILS

Crystal Growth

The crystals were grown by a two step halogen vapor transport method with Br_2 as the transporting agent. Small crystals were grown first from a stochiometric mixture of the powdered elements. The product of the first step became the starting material for the second growth which yielded crystals for study.

The starting materials together with the carrier substance were placed in a quartz ampoule (40 mm in diameter) which was then evaculated to a pressure about 10^{-6} torr and sealed. Crystal growth was conducted by inserting the filled ampoule in a horizontal tube furnace in which the appropriate temperatures and thermal gradients had been established, and leaving it undisturbed for a period of two to three weeks.

The crystal growth apparatus is shown in Fig. la. It consists essentially of a gradient furnace that permits careful control of the temperatures and temperature gradients in the regions of reaction and growth. The high temperature were provided by a Lindberg model 54259 three zone tube furnace with model 59495-A control console. A typical thermal gradient is shown in Fig. 1 b. Monitoring the temperature indicated that fluctuations in temperature were less than 1% during entire growing period. At the end of this period, the furnace was allowed to cool to about 500° C gradually. Then, the ampoule was
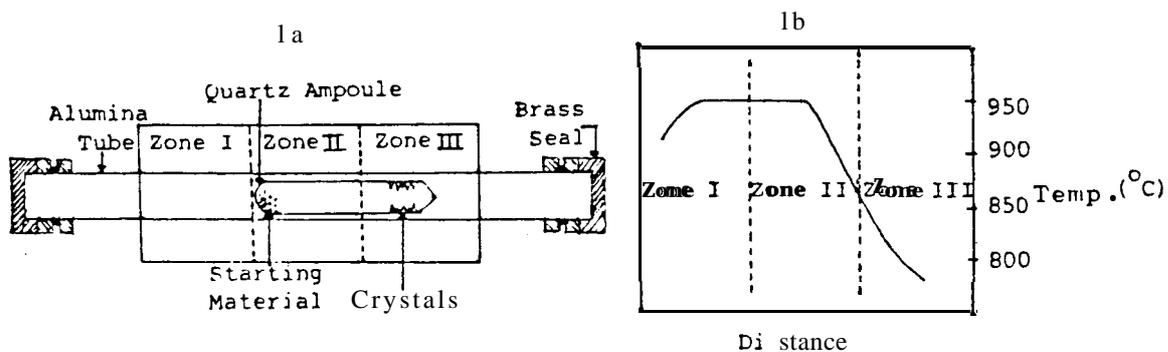

Fig. 1 Setup and temperature profile for the growth of MoSe$_2$ crystals.

moved and wet tissues were applied rapidly to the end away from the crystals to condense the Br_2 vapor. When the remainder of the ampoule had cooled to room temperature the ampoule was opened and the crystals which had grown at the cooler end were removed.

Conductivity Measurements

The temperature dependence of conductivity of ten samples from two different batches was studied bewteen $135°$ K and $800°$ K by using a four probe potentiometric technique[10] . The samples (thickness t) were cut into a rectangular shape of effective length l and width b. Electrical connections to the crystal were made by means of four parallel platinum wires laid across the basal surface of the thin crystal and attached to the crystal surface by means of conducting silver paint. The wires near each end of the rectangular crystal acted as current leads while the two contact wires (separation d) on either side of the centre line were used to measure the potential difference V in the crystal. With this electrode configuration the conductivity is σ defined by

$$\sigma = \frac{Id}{Vbt}$$

where I is the current through the sample from a constant current supply and the potential difference V, measured by a sensitive potentiometer, is the average value obtained on reversing the current through the sample. Dimensions d and b were measured by travelling microscope and the crystal thickness t by dial gauge.

Thermoreflectance[11]

As shown in Fig. 2, is a schematic drawing of the experimental arrangement for the TR
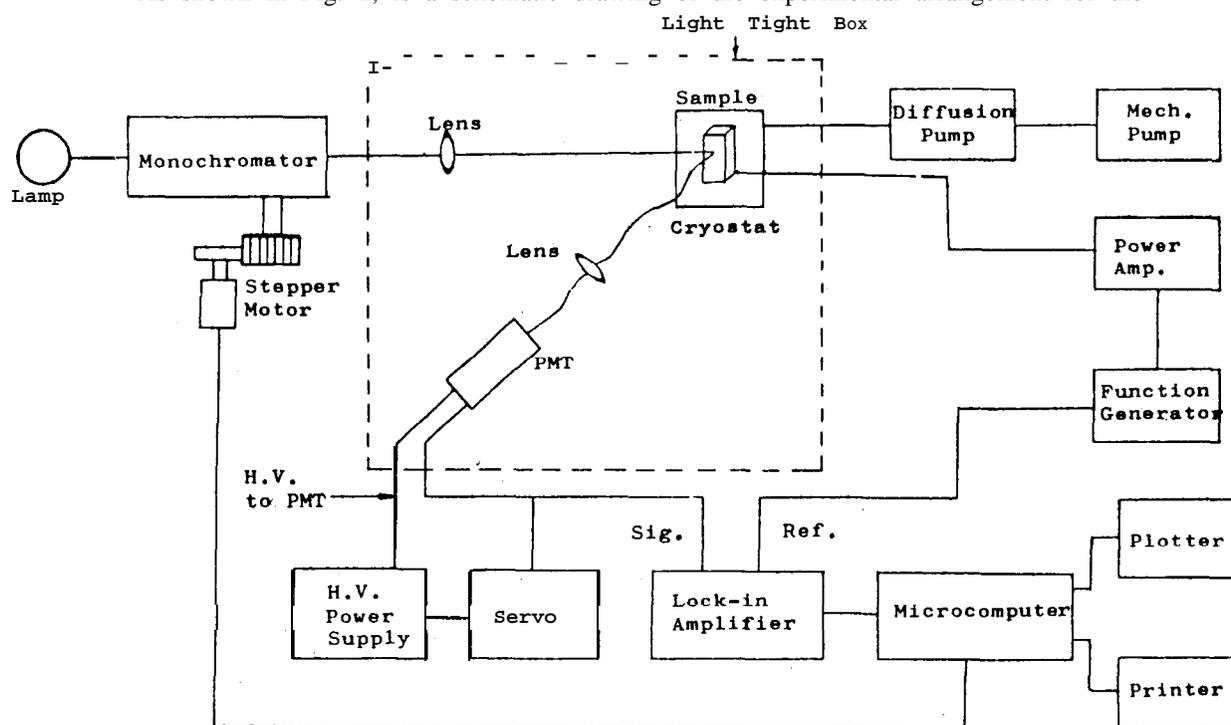

Fig. 2   Schematic diagram of the setup for thermoreflectance measurements.

measurements. Light from a xenon arc lamp is focused on the entrance slit of the monochromator. And the emergent monochromatic beam is focused on the sample from which it is reflected at near-normal incidence and directed onto a photomultiplier. .The samples were cut into thin rectangular pieces to reduce their heat capacity. Vacuum evaporated silver-electrodes were applied to the surface of the surface of the crystals on a plane perpendicular to the hexagonal c-axis. The sample was mounted on a thin layer of mylar with silicone vacuum grease for insulation and then was attached onto a copper heat sink. The temperature was modulated by passing a modulating pulse current (-10 Hz) directly through the samples. .The signal at the output of the photomultiplier contains two components: a dc part, $S = \gamma I_i R$, and a small ac component, $AS = \gamma I_i \Delta R$ where γ is the sensitivity of the photomultiplier; I_i, the incident light intensity; R, the reflectivity of the sample and AR is the change in the reflectivity of the sample caused by the temperature modification. The quantity of interest is the relative reflectivity, AR/R, which is related to the relative signal. It is apparent that

$$\frac{AS}{S} = \frac{\gamma I_i \Delta R}{I_i R} = \frac{\Delta R}{R}$$

The dc output, S, is maintained constant throughout the experiment by a servomechanism which controls the high voltage applied to the photomultiplier. The ac component, AS, is detected by the lock-in amplifier. Under these conditions the output from lock-in amplifier which goes to a microcomputer, is directly proportional to AR/R.

Electrolyte Electroreflectance

The electrolyte electroreflectance (EER) technique has been described extensively in the literature[12,13] The MoSe$_2$ electrode were prepared in the following way: The crystals were mounted on a copper plate and glued with conducting silver paint. One end of the copper plate was soldered to a copper wire which passed through a pyrex tube. The wires and plate were insulated with ordinary epoxy cement, leaving only the basal face exposed to the electrolyte. The electrolyte was a 3 wt.% tartaric acid solution mixed in the ratio 1:2 with ethylene glycol. The modulating voltage was in the form of a square wave, 100 mV peak to peak at 100 Hz. A dc bias of 0.1 V, positive with respect to the platinum counter electrode, was also applied to the sample.

3. RESULTS AND DISCUSSIONS

Crystal Growth

The halogen gases are best suited as transporting agents for the chalcogenides[14]. We have employed Bra for the growth of MoSe$_2$ crystals. The chemical reaction is

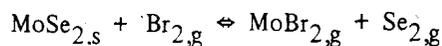$$MoSe_{2,s} + Br_{2,g} \Leftrightarrow MoBr_{2,g} + Se_{2,g}$$

Fig. 3 shows the crystals grown in our laboratory. Crystals as large as 10 x 10 x 1 mm^3 with mirror-like surface are obtained on a routine basis. The surfaces of these crystals showed well defined hexagonal growth spirals, as shown in Fig. 4. The success in growing large single crystals of MoSe$_2$ is based on the use of a two-step process, in which the initial step served to purify the starting materials. It also

produces a more compact starting materials. In the second step, the nucleation is less than in the original growth, and hence much larger crystals appeared. Crystals were grown in a variety of temperatures, temperature gradients and Br_2 concentrations. The optimum conditions are: The reaction temperature is about $960°C$, the growth temperature is in the range of $800°C$ to $840°C$, and the Br_2 concentrations is 2 mg/cm^3. The crystal structure was studied by x-ray powder diffraction and **was** confirmed to have 2H form.
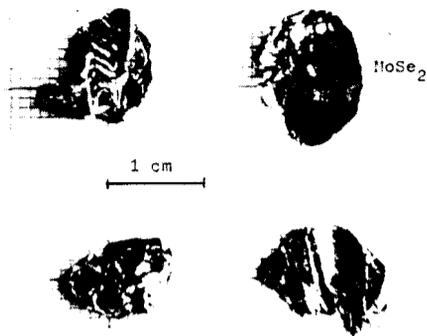

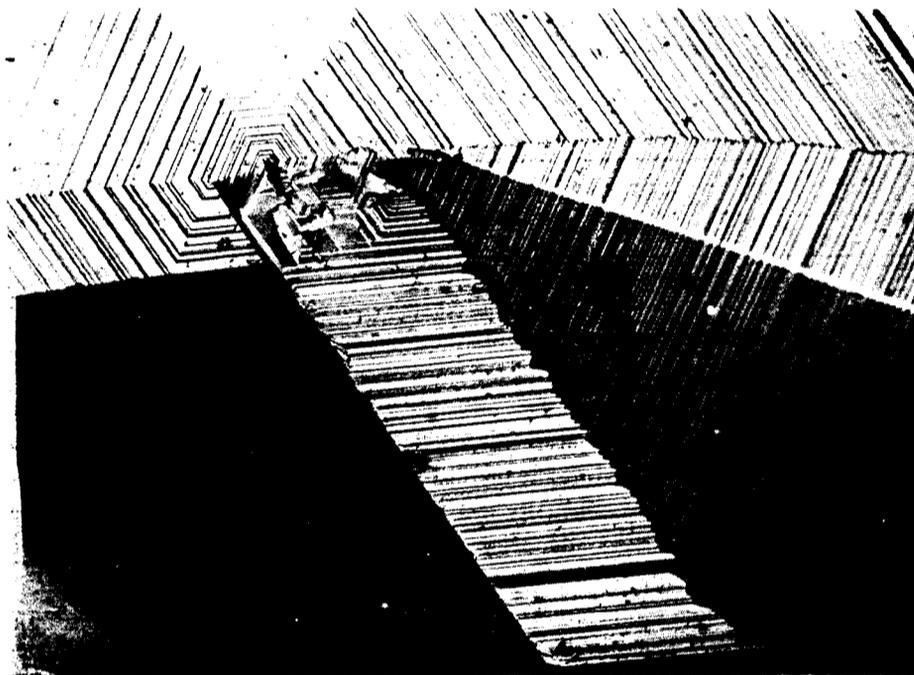Fig. 3 Some representative crystals of $MoSe_2$ grown in our laboratory.

Fig. 4 The hexagonal growth spirals on the surfaces of $MoSe_2$ crystals.
(magnification: 96 times)

Conductivity

Fig. 5 shows measured values of conductivity, σ, over the temperature range $135°$ K to $800°$ K for

two different samples of 2H-MoSe$_2$. The curve labeled, (a), is for the sample grown from the constituent elements.. The curve labeled, (b), is for the sample grown from small crystals. Both crystals are n-type at room temperature.
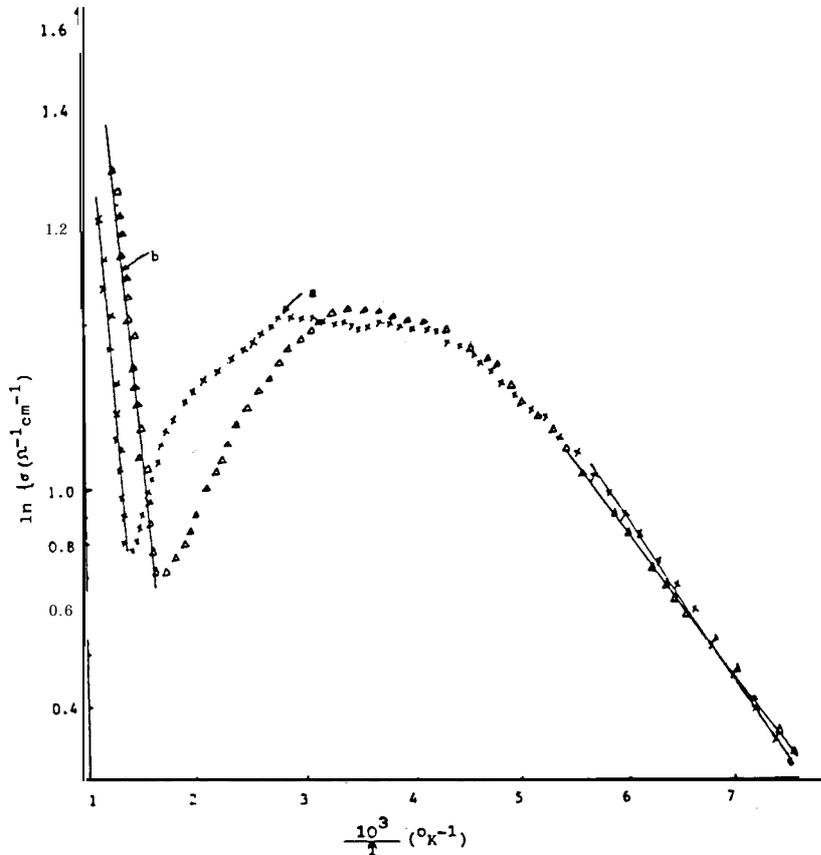

Fig. 5 The electrical conductivity $\sigma(\Omega^{-1}cm^{-1})$ versus $10^3/T(^{\circ}K^{-1})$
for two different single crystals of n-MoSe$_2$.
(a) crystal grown from the constituent elements
(b) crystal grown from small crystals

For sample (a), at room temperature the conductivity, σ, is $1.08\Omega^{-1}cm^{-1}$. Curve (a) shows two linear regions. Below room temperature the thermal activation energy was 0.148 ± 0.04 eV. At temperatures above 700° K the electrical conductivity increases rapidly with rising temperature. This behavior is attributed to the onset of intrinsic conductivity. From the slope of the linear portion of the $\ln\sigma$ versus ·1000/T graph. the thermal energy gap is computed to be 1.006 ± 0.04 eV.

For sample (b), at room temperature the conductivity, σ, is $1.02\Omega^{-1}cm^{-1}$. The $\ln\sigma$ versus 1000/T graph again shows two linear regions: Below room temperature the thermal activation energy $E_a = 0.142 \pm 0.04$ eV while above 650° K the slope of the $\ln\sigma$ versus 1000/T graph gives $E_g = 0.990 \pm 0.04$ eV.

Comparing these two curves we observe that sample' (b) reaches the intrinsic region at a substantially lower temperature. It is evident from this that crystals grown from small crystals rather than from a stoichiometric mixture of the elements are of higher purity.

Fig. 5 indicated that the $\ln\sigma$ versus 1000/T plots, can be divided into three segments: a " low" temperature region having a portion with a slope corresponding to an activation energy of around 0.145

eV; a high temperature region with a steeper slope corresponding to an activation energy of around 0.5 eV; and a relatively fat intermediate portion connecting these two segments. The temperature ranges where these various regions occur differ from the sample to sample depending to some degree on the starting material for crystal growth..

In the low temperature region, below $200°K$ the slope corresponds to an energy of 0.145 eV which is probably the result of impurity activation. El-Mahalawy and Evans [10] found a value of 0.14 eV which they suggest could be the result of intrinsic conduction processes in the crystal. Fivaz and Mooser [15] reported that $MoSe_2$ became intrinsic at 200° K with a thermal band gap between 0.14 and 0.32 eV.

Our observations in the high temperature region are similar to those of other investigators. Above 650° K the $\ln\sigma$ vs $1000/T$ curve yields a thermal band gap, $E_g = 1.0$ eV. Evans and Hazelwood [16] reported measurements on n-type $MoSe_2$ crystals grown directly from the vapor of $E_g = 1.1$eV in the temperature range above 700° K. El-Mahalawy and Evans" reported 0.95 eV which they claimed represents the indirect band gap.

Thermoreflectance and Electrolyte Electroreflectance

The TR and EER spectrum of $MoSe_2$ at room temperature in the range of 1.4 to 6.2 eV are shown in Fig. 6 and Fig. 7, respectively. The structures have been labeled according to the commonly used notation for the transition-metal dichalcogenide compounds. Both TR and EER spectrum show sharp structures in the vicinity of the excitonic A, B, A' and B' as well as higher lying interband transitions. It is well established that minima in TR spectra correspond to inflexion points in the reflectivity spectra" and thus can be related to maxima in the absorption spectra' *. The EER spectrum contains features differing significantly in the structure from these of the TR spectrum, but which occur approximately
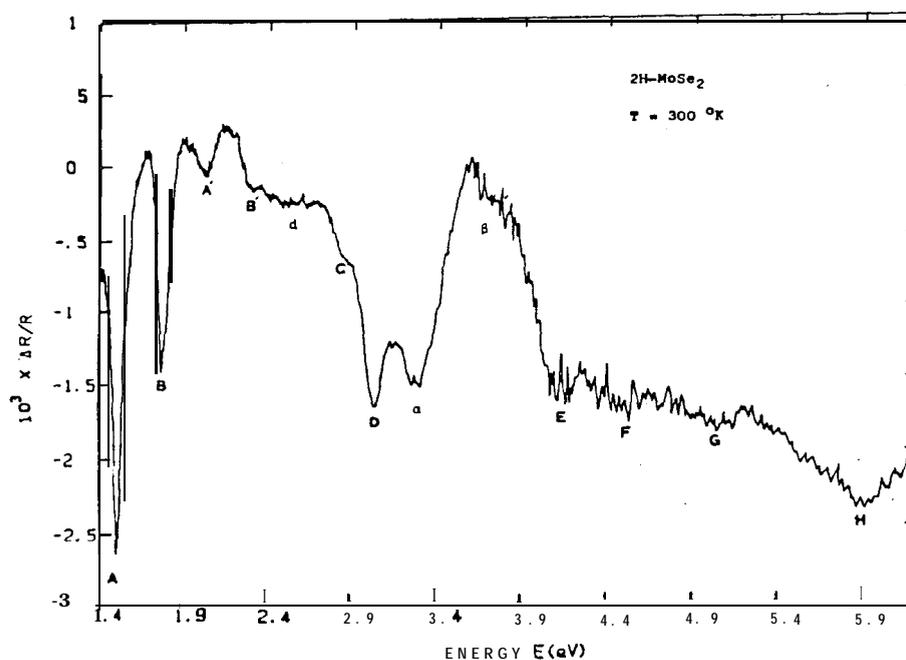

Fig. 6 The TR spectrum of 2H-$MoSe_2$ in the range of 1.4 to
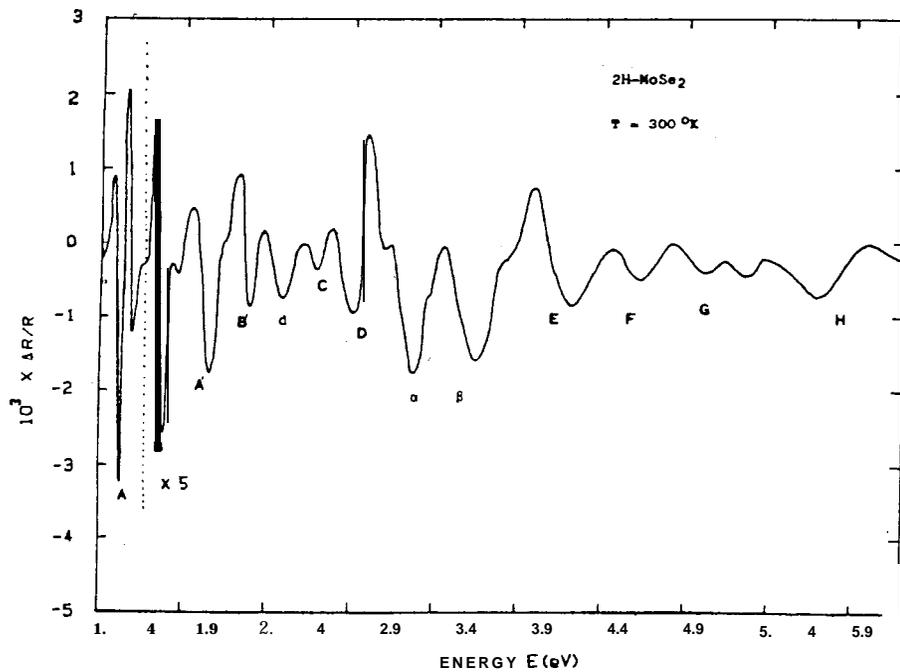6.2 eV at room temperature.

Fig. 7 The EER spectrum of 2H-MoSe$_2$ in the range of 1.4 to
6.2 eV with $\vec{E} \perp \vec{C}$ at room temperature.

at the same spectral locations. By the " three-point method" " we can determine the position of the inter-band transitions and the accuracy is better than 5 meV. Table 1 shows the energy position from the TR and EER spectrum. The energy positions found by reflectance (R) also shown in table 1 for comparison. This comparison helps to identify. the various features in the spectrum.

Table 1

A comparison of the energy positions of the various
features in the TR, EER and R[17] spectra.

Feature	Energy (eV)		
	TR	EER	R[17]
A	1.522	1.544	1.51
B	1.774	1.785	1.74
A'	2.028	2.062	2.05
B'	2.306	2.311	2.20
d	2.557	2.564	2.63
C	2.783	2.767	2.77
D	3.021	2.988	2.95
α	3.27	3.264	3.22
β	3.53	3.552	3.64
E	4.09	4.113	4.07
F	4.46	4.481	
G	5.05	5.102	
H	5.81	5.796	5.84

In order to interpret the presence of so many features, it is necessary to look into the band structure of $MoSe_2$. The only band calculation available for $MoSe_2$ were those of Bromley et al.[20] performed in the ideal two-dimensional model with the tight binding approximation. This model, however, is unable to explain the result that indirect rhermal band gap is around 1 eV. Mattheiss[21] in his augmented-plane wave (APW) method calculation of $MoSe_2$ indicates there is a 0.8 eV gap between the topmost d-like valence band and the lower p-like valence band this failed to predict the photoemission results[22] which probes the valence band directly and indicates that there is an overlap between the p and d subband of 0.5 eV. In the APW calculations the A, B, A' and B' excitons are due to d-d transitions which are allowed at the point $\vec{\Gamma}$. This is contrary to the recent Piezo-reflectance measurement reports[7,8] which indicate that A, B excitons and the A!, B' excitons have different origins. On the other hand the linear combination of muffin-tin orbitals (LCMTO) calculations made by Kasowski[23] for MoS_2 and NbS_2 are in good agreement with experiments (absorption[18] and photoemission[22]). Those compounds belong to tne same symmetry group $D_{6h}^{'4}$ as $MoSe_2$. Therefore, we choose to use the Kasowski' s model as a guide to determine the level sequence in $MoSe_2$.

Because of high atomic number of both constituents of the compound, spin-orbit splitting will play an important role in the band structure of $MoSe_2$. First, to include the effects of spin orbit splitting, the character table[24] is extended to the double group resulting in the correspondence shown in Fig. 8.
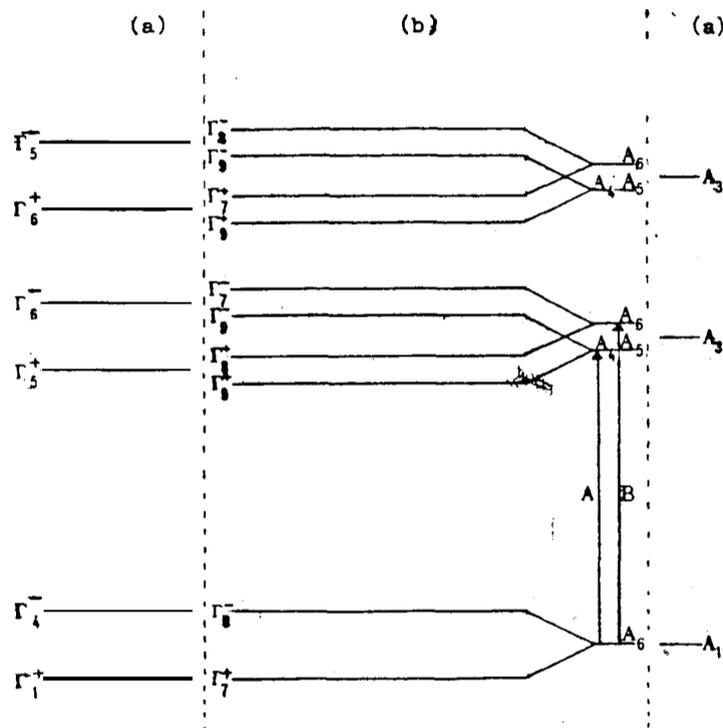

Fig. 8 Band sequence at $\vec{\Gamma}$ and $\vec{A}$ in 2H-$MoSe_2$

Fig. 8 gives schematically the sequence of the states at $\vec{\Gamma}$ and $\vec{A}$ including splitting by spin-orbit coupling. Bands splits at $\vec{\Gamma}$ by interlayer coupling are still degenerate at point $\vec{A}$. In Kasowski' s band scheme, optical transitions from the d_{z^2} (A,) band into the lower non-bonding band are allowed. The conduction states are split by spin-orbit coupling ($A_3 \to A_6 + A_4$, As). The symmetry selection rules allow two transitions. We attributed the A, B excitons to these transitions. The A' , B' excitons results from the transition $d_{z^2} \to d$ at the point $\vec{H}$ of the Brillouin zone. The C exciton results from the transition $d_{z^2} \to d/p$ along

the direction Δ near the point $\vec{A}$ and D results from the transition $d_{z^2} \rightarrow$ d/p along the direction P near the point $\vec{H}$. The α, β peaks result fro," the p $\rightarrow$ d/p trasition along the direction A near the point $\vec{A}$. The ' E feature results from transition at L and the F feature from either $\vec{L}$ or $\vec{A}$. The origin of the features d, G, H are also assumed to arise from interband transitions. The results of this study do not directly indicate the exact transitions associated with each feature but eventually help in this respect.

4. CONCLUSIONS

A " two-step" halogen vapor transport method has been developed for growing large size crystals of 2H-MoSe$_2$. Conductivity measurements show that intrinsic conductivity begins to dominate at 650° K with a thermal energy gap around 1 eV. The measurements of TR and EER spectrum of these crystals have enabled us to identify the various features in the spectrum and determine their interband transition energies with a better accuracy.

ACKNOWLEDGEMENT

REFERENCES

R. B. Somoano and A. Rambaum, Phys. Rev. Lett. 27,402 (1972).

2. D. W. Bullett, J. Phys. C : Solid State Phys. 11, 4501 (1978).
3. H. Tributsch, Solar Energy Material 1,257 (1979).
4. J. A, Wilson and A. D. Yoffee, Adv. Phys. 18, 193 (1969).
5. B. L. Evans, in Physics and Chemistry of Materials with Layered Structures, Vol. 4 : Electrical and Optical Properties, ed. by P. A. Lee, D. Reidel Publish, Boston (1976).
6. A. Anedda and E. Fortin, Phys. Chem. Solids 4 1,865 (1980).
7. K. Saiki, M. Yoshimi and S. Tanaka, phys. stat. sol.(b) 88,607 (1978).
8. M. Tanaka, H. Fukutani and G. Kuwabara, J. Phys. Soc. Japan 45, 1899 (1978).
9. H. Meinhold and G. Weiser, phys. stat. sol. (b) 73, 105 (1976).
10. S. H. El-Mahalawy and B. L. Evans, phys. stat. sol. (b) 79,713 (1977).
11. B. Batz, Semiconductors and Semimetals Vol. 9, eds. by R. L. Willardson and A. C. Beer, Academic Press, New York, 3 16 (1972).
12. D. E. Aspnes, Handbook on Semiconductors, Vol. 2, ed. by M. Balkanski, North Holland, Amsterdam, 109 (1980).
13. Y. Hamakawa and T. Nishino, Optical Properties of Solids : New Developments, ed. by B. 0. Seraphin, North Holland, Amsterdam, 255 (1976).
14. H. Schaffer, Chemical Transport Reactions, Academic Press, New York (1964).
15. R. Fivaz and E. Mooser, Phys. Rev. 163,743 (1967).
16. B. L. Evans and R. A. Hazelwood, phys. stat. sol. (a) 4,181 (1971)
17. P. M. Amirtharaj, F. H. Pollak and A. Wold, Solid State Comm. 41,581 (1982).
18. A. R. Beal, J. C. Knights and W. Y. Liang, J. Phys. C : Solid State Phys. 5, 3540 (1972).
19. D. E. Aspnes and J. E. Rowe, Phys. Rev. Lett. 27,188 (1971).

20.   R. A. Bromley, R. B. Murray and A. D. Yoffe, J. Phys. C : Solid State Phys. 5,759 (1972).

21.   L. F. Mattheiss, Phys. Rev. Lett. 30, 784 (1973).

22.   J. C. McMenamin and W. E. Spicer, Phys. Rev. B16, 5474 (1977).

23.   R. V. Kasowski, Phys. Rev. lett. 30, 1175 (1973).

24.   J. F. Cornwell, Group Theory and Electronic Energy Bands in Solids, John Wiley & Sons, New York (1969).